



Adaptive Neural Network-based Nonlinear Fault-Tolerant Control of a Disturbed UAV

Olivier Baraka Mushage

Associate Professor, Faculty of Applied Sciences and Technologies, Université Libre des Pays des Grands Lacs

ABSTRACT: This paper addresses the control problem for a six degree of freedom quadrotor subject to perturbations such as multiple actuation failures, external disturbances and uncertain parameters. A nonlinear control law is designed so that it provides a continuous control signal that tackles simultaneously the aforementioned perturbations. Through a Lyapunov stability analysis, it is proved that, under the proposed control law, stability of the closed-loop system and achievement of the control objectives are guaranteed. To illustrate the efficiency of the proposed quadrotor's controller, simulation results are presented. The obtained results are compared to those obtained using a controller available in the literature. Thanks to these results, robustness, fast response and good tracking capability guaranteed by the proposed controller are demonstrated. Hence, with the proposed controller, increased safety and reliability are obtained for the aircraft's operations.

KEYWORDS: Quadrotor, actuator fault, adaptive nonlinear control, neural network, parametric uncertainty, external disturbances.

I. INTRODUCTION

Drones are becoming popular as they are increasingly used in many applications such as environment exploration, military missions, traffic surveillance, rescue operations, structure inspection, mapping, aerial cinematography, parcel delivery, etc. [1-6]. Drones are multirotor Unmanned Aerial Vehicle (UAV) of different kinds like bi-rotor, tri-rotor, quadrotor, and conventional helicopter [3,6-8]. Since several years, a tremendous effort has been devoted to developing control strategies for different kinds of UAVs, which are highly nonlinear under-actuated systems. These UAVs are often affected by various disturbances, which makes their control very challenging. To accomplish efficiently their missions, these UAVs require controllers that can tackle actuation faults, environmental disturbances such as wind, rain and physical parameter changes such as variation of mass and inertia. UAVs can encounter loss of effectiveness (LOE) due to a motor's fault or propeller's damage or battery drainage [2, 3]. A partial LOE in one of the motors or in more causes simultaneous loss of thrust and torque. The occurrence of such faults significantly degrades the performance of the quadrotor. Fault-tolerant control (FTC) strategies are hence developed to accommodate such faults. Numerous papers proposing controllers for UAV with perturbations have been published. An FTC for a quadrotor has been presented in [7], which is based on the combination of the traditional sliding mode control (SMC) technique with the interval type-2 fuzzy logic control approach. The authors of [7] used the interval type-2 fuzzy system to cancel the chattering phenomenon, which is the main drawback of the SMC. However, the controller's implementation requires the exact knowledge of the UAV's parameters and the upper bound of a lumped disturbance. Robust controllers based on a second order SMC (SOSMC) strategy for a quadrotor UAV were proposed in [1]. The controllers were designed by considering separately a fully actuated subsystem and an underactuated subsystem. A sliding manifold that linearly combines tracking errors on two state variables and their derivatives was used for the design of a controller for the underactuated subsystem. However, exact knowledge of system parameters is necessary for the controllers' implementation. In [2], linear parameter varying (LPV) control technique was used to develop an active FTC strategy for a quadrotor. In addition to actuation faults, perturbations such as payload grasping and dropping caused variations of system dynamics were addressed. The proposed FTC uses an LPV-based fault detection and diagnosis (FDD) scheme that provides an estimated value of partial loss of effectiveness, which is used by the controller to compensate the effects of system parameters changes and actuation faults. However, this FTC is designed using a simplified linear model. Therefore, knowing that the quadrotor is a highly nonlinear system, the FTC controls it with limited accuracy. In addition, the use of the FDD increases computation burden and the risk of more tracking error in case of inaccurate fault estimation.

Motivated by the above discussion, considering that safety and reliability are always a critical issue for aircraft applications, this paper presents the design of an adaptive controller for a six degree of freedom quadrotor aircraft so that severe perturbations such as motors failures or rotor damages, unknown/uncertain parameters and external disturbances are tackled. This controller is based on the nonlinear control approach introduced in [9, 10] for strict-feedback nonlinear systems and it uses radial basis function neural networks (RBFNN) for unknown dynamics



approximation. Control signals generated are continuous so that real-world implementation can be possible with energy consumption reduction. To design controllers for the position subsystem, which is underactuated, virtual control inputs are designed for the x and y subsystem.

The paper is organized as follows: In section 2, the dynamic model for the quadrotor, is presented. The control problem is presented in section 3. Section 4 is devoted to the control law design and the Lyapunov's stability analysis for the controlled quadrotor by considering that its model is made of a set of coupled nonlinear subsystems. In section 5 simulation results are presented and discussed and a benchmark is presented. Section 6 concludes the paper.

II. QUADROTOR MODEL PRESENTATION

As aforementioned, a quadrotor UAV is a highly nonlinear, multivariable, and underactuated dynamic system.

Remark 1: Throughout all the paper, in order to alleviate notations, time varying quantities are written without the independent variable (t).

The complete dynamics that governs the quadrotor UAV can be obtained using the Newton-Euler approach as follows [1, 11]:

$$\left\{ \begin{array}{l} \ddot{x} = -\frac{k_1}{m_s} \dot{x} + \frac{1}{m_s} (\cos \phi \sin \theta \cos \psi + \sin \phi \sin \psi) u_1 \\ \ddot{y} = -\frac{k_2}{m_s} \dot{y} + \frac{1}{m_s} (\cos \phi \sin \theta \sin \psi - \sin \phi \cos \psi) u_1 \\ \ddot{z} = -g - \frac{k_3}{m_s} \dot{z} + \frac{1}{m_s} (\cos \phi \cos \psi) u_1 \\ \ddot{\phi} = qr \frac{I_y - I_z}{I_x} + \frac{J_r}{I_x} q \Omega_r - \frac{k_4}{I_x} l p + \frac{l}{I_x} u_2 \\ \ddot{\theta} = pr \frac{I_z - I_x}{I_y} - \frac{J_r}{I_y} p \Omega_r - \frac{k_5}{I_y} l q + \frac{l}{I_y} u_3 \\ \ddot{\psi} = pq \frac{I_x - I_y}{I_z} - \frac{k_6}{I_r} r + \frac{C}{I_z} u_4 \end{array} \right. \quad (1)$$

where:

- $[x, y, z]^T$ is the quadrotor's center of gravity (COG) position vector in the earth-frame;
- $[\phi, \theta, \psi]^T$ is the vector of the three Euler's angles, which are the roll, the pitch and the yaw, respectively;
- $[p, q, r]^T$ is the angular velocity vector in the body frame;
- $k_i > 0$, is the air drag coefficient in the i th degree of freedom ($i = 1, 2, 3, 4, 5, 6$);
- J_r is the inertia of the z -axis;
- g is the acceleration of gravity;
- l is the distance from the center of each rotor to the COG;
- $C > 0$ is a proportional coefficient;
- I_x, I_y et I_z are the inertia of the quadrotor in the e_x, e_y and e_z axis, respectively;
- u_1 is the total thrust on the body in the z -axis;
- u_2, u_3 and u_4 are the roll torque, the pitch torque and the yawing torque, respectively;
- $\Omega_r = -\Omega_1 + \Omega_2 - \Omega_3 + \Omega_4$ is the overall residual rotor angular velocity with Ω_i being the angular velocity of the i th rotor ($1 \leq i \leq 4$).

In Eq. (1), the terms $K_1 \dot{x}/m_s$, $K_2 \dot{y}/m_s$ and $K_3 \dot{z}/m_s$ represent air drag distribution in the e_x, e_y and e_z axis, respectively.

Assumption 1: There is no singularity problem as the Euler's angles are bounded as follows: the roll angle, $-\pi/2 < \phi < \pi/2$; the pitch angle, $-\pi/2 < \theta < \pi/2$; and the yaw angle, $-\pi < \psi < \pi$.

The angular velocity vector in the body frame is related to the Euler's angles as follows:

$$\begin{bmatrix} p \\ q \\ r \end{bmatrix} = \begin{bmatrix} 1 & \sin \phi \tan \theta & \cos \phi \tan \theta \\ 0 & \cos \phi & -\sin \phi \\ 0 & \sin \phi \sec \theta & \cos \phi \sec \theta \end{bmatrix} \begin{bmatrix} \dot{\phi} \\ \dot{\theta} \\ \dot{\psi} \end{bmatrix} \quad (2)$$



Assumption 2: The quadrotor is considered being asymmetric rigid body.

For each of the four rotors, the angular velocity Ω_i is related to the control input u_i (for $1 \leq i \leq 4$) as follows:

$$\begin{bmatrix} u_1 \\ u_2 \\ u_3 \\ u_4 \end{bmatrix} = \begin{bmatrix} b & b & b & b \\ lb & 0 & -lb & 0 \\ 0 & -lb & 0 & lb \\ -k & k & -k & k \end{bmatrix} \begin{bmatrix} \Omega_1^2 \\ \Omega_2^2 \\ \Omega_3^2 \\ \Omega_4^2 \end{bmatrix} \tag{3}$$

where $k > 0$ and $b > 0$ are parameters depending on the density of air, the radius of the propellers, the number of blades, their geometry, and their lift and drag coefficients [1, 12].

The thrust generated by the i th (with $i = 1, 2, 3, 4$) rotor is given by:

$$F_i = b\Omega_i^2 \tag{4}$$

The thrusts F_i (with $i = 1, 2, 3, 4$) are considered as the real control inputs to the dynamical system. The reactive torque caused by the rotor drag generated by the rotation of the i th rotor in free air is:

$$M_i = -k\Omega_i^2 \tag{5}$$

The rolling torque is provided by the difference between the first and third rotors' thrusts as follows:

$$M_\phi = l(F_1 - F_3) \tag{6}$$

The pitching torque is due to the difference between the thrusts generated by the second and the fourth rotor as follows:

$$M_\theta = l(F_4 - F_2) \tag{7}$$

The yawing torque generated by the four rotors is:

$$M_\psi = C(F_1 - F_2 + F_3 - F_4) \tag{8}$$

III. PROBLEM STATEMENT

Let us consider a quadrotor UAV with uncertain parameters (i.e. with modelling errors and/or random parameters changes), external disturbances on the six degrees of freedom and actuation faults. Therefore, the UAV is modelled as a set of the following subsystems:

(a) **The roll (ϕ), pitch (θ) and yaw (ψ) subsystem**

$$\begin{cases} \dot{X}_{1,\phi,\theta,\psi} = X_{2,\phi,\theta,\psi} \\ \dot{X}_{2,\phi,\theta,\psi} = f_{\phi,\theta,\psi}(X) + b_{\phi,\theta,\psi}u_{\phi,\theta,\psi} + d_{\phi,\theta,\psi} \end{cases} \tag{9}$$

(b) **The x and y positions subsystem**

$$\begin{cases} \dot{X}_{1,x,y} = X_{2,x,y} \\ \dot{X}_{2,x,y} = f_{x,y}(X) + b_{x,y}u_{x,y} + d_{x,y} \end{cases} \tag{10}$$

(c) **The altitude (z) subsystem**

$$\begin{cases} \dot{x}_{11} = x_{12} \\ \dot{x}_{12} = a_{11}x_{12} - g + \frac{g_z(X)}{m_s}u_1 + d_z \end{cases} \tag{11}$$

where :

$$\begin{aligned} X &= [x_1, x_2, x_3, x_4, x_5, x_6, x_7, x_8, x_9, x_{10}, x_{11}, x_{12}]^T = [\phi, \dot{\phi}, \theta, \dot{\theta}, \psi, \dot{\psi}, x, \dot{x}, y, \dot{y}, z, \dot{z}]^T, \\ X_{1,\phi,\theta,\psi} &= [x_1, x_3, x_5]^T, X_{2,\phi,\theta,\psi} = [x_2, x_4, x_6]^T, X_{1,x,y} = [x_7, x_9]^T, X_{2,x,y} = [x_8, x_{10}]^T, \\ f_{x,y}(X) &= [a_9x_8, a_{10}x_9]^T, f_{\phi,\theta,\psi}(X) = \begin{bmatrix} a_1qr + a_2q\Omega_r + a_3p \\ a_4pr + a_5p\Omega_r + a_6q \\ a_7pq + a_8r \end{bmatrix}, b_{\phi,\theta,\psi} = \text{diag}[b_1, b_2, b_3], \end{aligned}$$



$$\begin{aligned}
 \mathbf{b}_{x,y} &= \text{diag}[1/m_s, 1/m_s], \mathbf{u}_{\phi,\theta,\psi} = [u_2, u_3, u_4]^T, \mathbf{u}_{x,y} = [u_x, u_y]^T, a_1 = \frac{l_y - l_z}{l_x}, a_2 = \frac{l_r}{l_x}, a_3 = -\frac{k_4}{l_x} l, \\
 a_4 &= \frac{l_z - l_x}{l_y}, a_5 = -\frac{l_r}{l_y}, a_6 = -\frac{k_5}{l_y}, a_7 = \frac{l_x - l_y}{l_x}, a_8 = -\frac{k_6}{l_z}, a_9 = -\frac{k_1}{m_s}, a_{10} = -\frac{k_2}{m_s}, a_{11} = -\frac{k_3}{m_s}, b_1 = \frac{l}{l_x}, \\
 b_2 &= \frac{l}{l_y}, b_3 = \frac{c}{l_z}, g_z(\mathbf{X}) = \cos x_1 \cos x_3, u_x = \cos x_1 \sin x_3 \cos x_5 + \sin x_1 \sin x_5, \\
 u_y &= \cos x_1 \sin x_3 \sin x_5 - \sin x_1 \cos x_5, d_j \text{ (with } j = x, y, z, \phi, \theta, \psi) \text{ is an unknown bounded} \\
 &\text{external disturbance affecting the } j \text{ movement and } u_i \text{ (with } 1 \leq i \leq 4) \text{ is an actuator's output} \\
 &\text{modelled as follows [9, 10, 13]:} \\
 u_i &= (1 - g_{ia})u_{ia} + b_{ia}, \forall t \geq t_f \tag{12}
 \end{aligned}$$

where u_{ia} is the i th actuator's input, $0 \leq g_{ia} < 1$ is the degree to which the actuator's effectiveness is lost, b_{ia} is the bias fault and t_f is the unknown fault occurrence time. Hence, the actuator's fault can be either a constant/time varying nonaffine fault (when $1 - g_{ia} \neq 0$), a bias fault (when $u_i = u_{ia} + b_{ia}$), a gain fault (when $u_i = (1 - g_{ia})u_{ia}$) or a complex fault corresponding to the combination of all the aforementioned faults. The control objective is to apply suitable control actions to the four rotors of the UAV such that the quadrotor remains stable while tracking $x_{1d}, x_{3d}, x_{5d}, x_{7d}, x_{9d}$ and x_{11d} , which are the desired values for angles ϕ, θ, ψ and positions x, y and z , respectively. This control objective should be achieved despite perturbations such as external disturbances, uncertain parameters and multiple actuation faults.

IV. DESIGN OF THE ADAPTIVE RBFNN-BASED FAULT-TOLERANT CONTROLLER

Let us define $\mathbf{e} = [e_\phi, e_\theta, e_\psi, e_x, e_y, e_z]^T$ as the tracking error vector for the six subsystems with:

$$\begin{cases} e_\phi = x_1 - x_{1d} \\ e_\theta = x_3 - x_{3d} \\ e_\psi = x_5 - x_{5d} \\ e_x = x_7 - x_{7d} \\ e_y = x_9 - x_{9d} \\ e_z = x_{11} - x_{11d} \end{cases} \tag{13}$$

Let us define $\mathbf{s} = [s_z, s_\phi, s_\theta, s_\psi, s_x, s_y]^T$ as a vector of filtered errors functions, for the six subsystems, where:

$$s_j = \dot{e}_j + c_j e_j \tag{14}$$

with $c_j > 0$ and $j = \phi, \theta, \psi, x, y, z$.

The control law for the three aforementioned subsystems is designed as follows:

$$\mathbf{u}_a = \mathbf{G}(\mathbf{X})[-\widehat{\mathbf{F}}(\mathbf{X}_e|\widehat{\mathbf{W}}) - \widehat{\boldsymbol{\eta}}\mathbf{T}(\mathbf{s}) - \mathbf{K}\mathbf{E}(\mathbf{s})] \tag{15}$$

where $\mathbf{u}_a = [u_{a1}, u_{a2}, u_{a3}, u_{a4}, u_x, u_y]^T$, $\mathbf{G}(\mathbf{X}) = \text{diag}[1/g_z(\mathbf{X}), 1, 1, 1, 1/u_{a1}, 1/u_{a1}]$, $\widehat{\mathbf{F}}(\mathbf{X}) = [\hat{f}_z, \hat{f}_\phi, \hat{f}_\theta, \hat{f}_\psi, \hat{f}_x, \hat{f}_y]^T$, $\mathbf{T}(\mathbf{s}) = [T_z(s_z), T_\phi(s_\phi), T_\theta(s_\theta), T_\psi(s_\psi), T_x(s_x), T_y(s_y)]^T$, $\mathbf{E}(\mathbf{s}) = [E_z(s_z), E_\phi(s_\phi), E_\theta(s_\theta), E_\psi(s_\psi), E_x(s_x), E_y(s_y)]^T$, $T_j(s_j) = (e^{4s_j} - 1)/(e^{4s_j} + 1)$, $E_j(s_j) = s_j/(e^{4s_j} + 1)$, $j = \phi, \theta, \psi, x, y, z$, $\widehat{\boldsymbol{\eta}} = \text{diag}[\hat{\eta}_z, \hat{\eta}_\phi, \hat{\eta}_\theta, \hat{\eta}_\psi, \hat{\eta}_x, \hat{\eta}_y]$ given by

$$\begin{cases} \hat{\boldsymbol{\eta}} = \hat{\boldsymbol{\eta}}_1 + \boldsymbol{\eta}_2 \in \mathbb{R}^{6 \times 6} \\ \hat{\boldsymbol{\eta}}_1 = \text{diag}[\hat{\eta}_{1,z}, \hat{\eta}_{1,\phi}, \hat{\eta}_{1,\theta}, \hat{\eta}_{1,\psi}, \hat{\eta}_{1,x}, \hat{\eta}_{1,y}] \in \mathbb{R}^{6 \times 6} \\ \hat{\eta}_{1,k} = \Gamma_{\eta,k}^{-1} |\mathbf{s}_k| \in \mathbb{R}^{6 \times 6}, j = z, \phi, \theta, \psi, x, y \\ \dot{\hat{\boldsymbol{\eta}}} = \boldsymbol{\Gamma}_\epsilon^{-1} \mathbf{s} \in \mathbb{R}^{6 \times 6} \\ \boldsymbol{\eta}_2 = \text{diag}[\rho|\hat{\epsilon}_z|, \rho|\hat{\epsilon}_\phi|, \rho|\hat{\epsilon}_\theta|, \rho|\hat{\epsilon}_\psi|, \rho|\hat{\epsilon}_x|, \rho|\hat{\epsilon}_y|] \in \mathbb{R}^{6 \times 6} \end{cases} \tag{16}$$

with $\Gamma_{\eta,k} > 0$, $\boldsymbol{\Gamma}_\epsilon = \boldsymbol{\Gamma}_\epsilon^T > 0 \in \mathbb{R}^{6 \times 6}$ and $\rho > 1$.

$\widehat{\mathbf{F}}(\mathbf{X})$ is an approximation of the unknown system's dynamics, which is obtained using a RBFNN. A RBFNN is a feedforward 3-layer network that uses the universal approximation theorem to approximate any smooth function on a



compact set $\Omega \in \mathbb{R}^n$. RBFNNs have been used in many studies for their ability of accelerating learning speed and avoiding local minimum problem that make them suitable for real-time control systems with improved control accuracy, robustness and adaptability [13, 14, 15, 16]. The nonlinear function $\hat{F}(X)$ is obtained using:

$$\hat{F}(X) = \hat{W}^T h(X_e) \tag{17}$$

Where $X_e \in \mathbb{R}^6$ (with elements being $x_{e1} = [e_j, \dot{e}_j]^T$) is the set of RBFNN's input, $h(X_e) = [h_z^T(x_{ez}), h_\phi^T(x_{e\phi}), h_\theta^T(x_{e\theta}), h_\psi^T(x_{e\psi}), h_x^T(x_{ex}), h_y^T(x_{ey})]^T \in \mathbb{R}^{6m}$ with $h_j(X_{ej}) = [h_{j1}, h_{j2}, \dots, h_{jm}]^T$ being the radial basis vector function where :

$$h_{ji}(X_{ej}) = \exp\left(-\frac{\|x_{ej} - \lambda_i\|^2}{2\beta_i^2}\right) \tag{18}$$

with $\lambda = [\lambda_1, \lambda_2, \dots, \lambda_m]^T$ and $\beta = [\beta_1, \beta_2, \dots, \beta_m]^T$ being the centric vector and base width vector of the radial basis function, respectively, and $i = 1, 2, \dots, m$, m being the number of neurons in the hidden layer of the neural network (NN); and $\hat{W} \in \mathbb{R}^{6m \times 6}$ is obtained from:

$$\hat{W} = \Gamma^{-1} h(x_e) s^T \tag{19}$$

with $\Gamma = \Gamma^T > 0 \in \mathbb{R}^{6 \times 6}$.

The difference between the RBFNN output $\hat{F}(X_e | \hat{W})$ and the exact nonlinear function $F(X) = [f_z, f_\phi, f_\theta, f_\psi, f_x, f_y]^T$ is expressed as:

$$\hat{F}(X_e | \hat{W}) - F(X) = \hat{W}^T h(X_e) - \varepsilon(X_e) I_6 \tag{20}$$

where $I_6 \in \mathbb{R}^6$ is a unit column vector, \hat{W} is the error of weight matrix approximation and the RBFNN approximation error vector is $\varepsilon(X_e) = [\varepsilon_z, \varepsilon_\phi, \varepsilon_\theta, \varepsilon_\psi, \varepsilon_x, \varepsilon_y]^T$, which is assumed bounded by an unknown constant.

Theorem 1 By considering the quadrotor model expressed by Eqs. 9-11 with unknown parameters, actuation faults and external disturbances, by using the nonlinear control law expressed by Eq. (15), where the quantities expressed by Eqs. (16)-(19) are used, the quadrotor is stable and the control objective is achieved.

Proof First, let us set the following equality:

$$M \cdot \dot{X}_2 = F'(X) + G^{-1}(X) u_a + \xi(X, u_a) \tag{21}$$

where $M = \text{diag}[m_s, 1/b_1, 1/b_2, 1/b_3, m_s, m_s]$, $X_2 = [x_{12}, x_2, x_4, x_6, x_8, x_{10}]^T$, $\xi(X, u_a) = [\xi_z, \xi_\phi, \xi_\theta, \xi_\psi, \xi_x, \xi_y]^T$ and $F'(X) = [a_{11}x_{12} - g, a_1qr + a_2q\Omega_r + a_3p, a_4pr + a_5p\Omega_r + a_6q, a_7pq + a_8r, a_9x_8, a_{10}x_9]^T$.

The vector of filtered error functions, where Eqs.(15) and (20) are applied, can be expressed as follows:

$$\begin{aligned} M \cdot \dot{s} &= M\ddot{e} + M \cdot c \cdot \dot{e} \\ &= -[\hat{W}^T h(X_e) - \varepsilon(X_e) I_6] + \xi(X, u_a) - \hat{\eta}T(s) - KE(s) \end{aligned} \tag{22}$$

where the tracking error vector $e = X_1 - X_{1d} \in \mathbb{R}^6$ (with $\dot{X}_1 = X_2$, $X_1 = [x_{11}, x_1, x_3, x_5, x_7, x_9]^T$) and $X_{1d} \in \mathbb{R}^6$ is the vector of desired values for X_1) and the entries of the diagonal matrix c are $c_j > 0$ (with $j = \phi, \theta, \psi, x, y, z$). Knowing that

$$F(X) = F'(X) + M \cdot c \cdot \dot{e} - M\ddot{X}_{1d} \tag{23}$$

Let us now consider the following candidate Lyapunov function:

$$V = V_1 + V_2 \tag{24}$$



with

$$V_1 = \frac{1}{2} \mathbf{s}^T \mathbf{M} \mathbf{s} + \frac{1}{2} \text{tr}[\widetilde{\mathbf{W}}^T \Gamma \widetilde{\mathbf{W}}] \tag{25}$$

where the error on $\widetilde{\mathbf{W}}$ is defined as follows:

$$\widetilde{\mathbf{W}} = \widehat{\mathbf{W}} - \mathbf{W}^* \tag{26}$$

$\mathbf{W}^* \in \mathbb{R}^{6m \times 6}$ is the optimal weight matrix used hereonly for analytic purpose. Furthermore, by considering $\widehat{\boldsymbol{\eta}}_1 \mathbf{I}_6$ as an estimation of the lumped disturbance $\xi(\mathbf{X}, \mathbf{u}_a)$ such that the approximation error is

$$\widetilde{\boldsymbol{\eta}}_1 \mathbf{I}_6 = \widehat{\boldsymbol{\eta}}_1 \mathbf{I}_6 - \xi(\mathbf{X}, \mathbf{u}_a) \tag{27}$$

we formulate

$$V_2 = \frac{1}{2} \text{tr}[\widetilde{\boldsymbol{\eta}}_1^T \Gamma_\eta \widetilde{\boldsymbol{\eta}}_1] + \frac{1}{2} \widetilde{\boldsymbol{\varepsilon}}^T \Gamma_\varepsilon \widetilde{\boldsymbol{\varepsilon}} \tag{28}$$

where

$$\widetilde{\boldsymbol{\varepsilon}} = \widehat{\boldsymbol{\varepsilon}} - \boldsymbol{\varepsilon}(\mathbf{X}_e) \tag{29}$$

is a diagonal matrix of error on parameter $\widehat{\boldsymbol{\varepsilon}} \in \mathbb{R}^{6 \times 6}$ (the approximate RBFNN error).

The first derivative of V_1 with respect to time in which Eq. (26) is applied is:

$$\begin{aligned} \dot{V}_1 &= \mathbf{s}^T \mathbf{M} \dot{\mathbf{s}} + \text{tr}[\widetilde{\mathbf{W}}^T \Gamma \dot{\widetilde{\mathbf{W}}}] \\ &= \mathbf{s}^T \mathbf{M} \dot{\mathbf{s}} + \text{tr}[\widetilde{\mathbf{W}}^T \Gamma \dot{\widehat{\mathbf{W}}}] \end{aligned} \tag{30}$$

Using Eq. (22) and the update law given by (19) in Eq.(30) yields

$$\begin{aligned} \dot{V}_1 &= \mathbf{s}^T \{-[\widetilde{\mathbf{W}}^T \mathbf{h}(\mathbf{X}_e) - \boldsymbol{\varepsilon}(\mathbf{X}_e) \mathbf{I}_6] + \xi(\mathbf{X}, \mathbf{u}_a) - \widehat{\boldsymbol{\eta}}^T \mathbf{T}(s) - \mathbf{K} \mathbf{E}(s)\} + \text{tr}[\widetilde{\mathbf{W}}^T \Gamma \dot{\widehat{\mathbf{W}}}] \\ &= \text{tr}[\widetilde{\mathbf{W}}^T (\Gamma \dot{\widehat{\mathbf{W}}} - \mathbf{h}(\mathbf{X}_e)) \mathbf{s}^T] + \mathbf{s}^T \boldsymbol{\varepsilon}(\mathbf{X}_e) \mathbf{I}_6 + \mathbf{s}^T \xi(\mathbf{X}, \mathbf{u}_a) - \mathbf{s}^T \widehat{\boldsymbol{\eta}}^T \mathbf{T}(s) - \mathbf{s}^T \mathbf{K} \mathbf{E}(s) \end{aligned} \tag{31}$$

The first derivative of Eq. (28) with respect to time, in which the identities given by Eqs. (27) and (29) are applied, is obtained as follows:

$$\dot{V}_2 = \text{tr}[\widetilde{\boldsymbol{\eta}}_1^T \Gamma_\eta \dot{\widetilde{\boldsymbol{\eta}}_1}] + \widetilde{\boldsymbol{\varepsilon}}^T \Gamma_\varepsilon \dot{\widetilde{\boldsymbol{\varepsilon}}} = \text{tr}[\widetilde{\boldsymbol{\eta}}_1^T \Gamma_\eta \dot{\widehat{\boldsymbol{\eta}}_1}] + \widetilde{\boldsymbol{\varepsilon}}^T \Gamma_\varepsilon \dot{\widehat{\boldsymbol{\varepsilon}}} \tag{32}$$

Therefore, using Eqs. (31) and (32), by applying Eq.(29) and the update rule for parameter $\widehat{\boldsymbol{\varepsilon}}$ given by Eq.(16), the first-time derivative of the Lyapunov's function is obtained as follows:

$$\begin{aligned} \dot{V} &= \text{tr}[\widetilde{\mathbf{W}}^T (\Gamma \dot{\widehat{\mathbf{W}}} - \mathbf{h}(\mathbf{X}_e)) \mathbf{s}^T] + \mathbf{s}^T \boldsymbol{\varepsilon}(\mathbf{X}_e) \mathbf{I}_6 + \mathbf{s}^T \xi(\mathbf{X}, \mathbf{u}_a) - \mathbf{s}^T \widehat{\boldsymbol{\eta}}^T \mathbf{T}(s) - \mathbf{s}^T \mathbf{K} \mathbf{E}(s) + \text{tr}[\widetilde{\boldsymbol{\eta}}_1^T \Gamma_\eta \dot{\widehat{\boldsymbol{\eta}}_1}] + \widetilde{\boldsymbol{\varepsilon}}^T \Gamma_\varepsilon \dot{\widehat{\boldsymbol{\varepsilon}}} \\ &= \mathbf{s}^T (\widehat{\boldsymbol{\varepsilon}} - \widetilde{\boldsymbol{\varepsilon}}) \mathbf{I}_6 + \mathbf{s}^T \xi(\mathbf{X}, \mathbf{u}_a) - \mathbf{s}^T \widehat{\boldsymbol{\eta}}^T \mathbf{T}(s) - \mathbf{s}^T \mathbf{K} \mathbf{E}(s) + \text{tr}[\widetilde{\boldsymbol{\eta}}_1^T \Gamma_\eta \dot{\widehat{\boldsymbol{\eta}}_1}] + \widetilde{\boldsymbol{\varepsilon}}^T \Gamma_\varepsilon \dot{\widehat{\boldsymbol{\varepsilon}}} \tag{33} \\ &= \mathbf{s}^T \xi(\mathbf{X}, \mathbf{u}_a) - \mathbf{s}^T \widehat{\boldsymbol{\eta}}^T \mathbf{T}(s) - \mathbf{s}^T \mathbf{K} \mathbf{E}(s) + \text{tr}[\widetilde{\boldsymbol{\eta}}_1^T \Gamma_\eta \dot{\widehat{\boldsymbol{\eta}}_1}] + \mathbf{s}^T \widehat{\boldsymbol{\varepsilon}} \mathbf{I}_6 \end{aligned}$$

Considering that in case of a severe perturbation caused by the lumped disturbance $\xi(\mathbf{X}, \mathbf{u}_a)$ the variable \mathbf{s} diverges from the origin such that $T_i(s_i) \cong 1$, Eq. (33) can be rewritten as follows:

$$\begin{aligned} \dot{V} &\cong \mathbf{s}^T \xi(\mathbf{X}, \mathbf{u}_a) - \mathbf{s}^T \widehat{\boldsymbol{\eta}} \mathbf{I}_6 - \mathbf{s}^T \mathbf{K} \mathbf{E}(s) + \text{tr}[\widetilde{\boldsymbol{\eta}}_1^T \Gamma_\eta \dot{\widehat{\boldsymbol{\eta}}_1}] + \mathbf{s}^T \widehat{\boldsymbol{\varepsilon}} \mathbf{I}_6 \\ &= \mathbf{s}^T (\widehat{\boldsymbol{\eta}}_1 - \widetilde{\boldsymbol{\eta}}_1) \mathbf{I}_6 - \mathbf{s}^T (\widehat{\boldsymbol{\eta}}_1 + \boldsymbol{\eta}_2) \mathbf{I}_6 - \sum_{i=1}^6 K_i \frac{s_i^2}{\exp(s_i) + 1} + \text{tr}[\widetilde{\boldsymbol{\eta}}_1^T \Gamma_\eta \dot{\widehat{\boldsymbol{\eta}}_1}] + \mathbf{s}^T \widehat{\boldsymbol{\varepsilon}} \mathbf{I}_6 \tag{34} \\ &= \mathbf{s}^T \widetilde{\boldsymbol{\eta}}_1 \mathbf{I}_6 - \mathbf{s}^T \boldsymbol{\eta}_2 \mathbf{I}_6 - \sum_{i=1}^6 K_i \frac{s_i^2}{\exp(s_i) + 1} + \text{tr}[\widetilde{\boldsymbol{\eta}}_1^T \Gamma_\eta \dot{\widehat{\boldsymbol{\eta}}_1}] + \mathbf{s}^T \widehat{\boldsymbol{\varepsilon}} \mathbf{I}_6 \end{aligned}$$

where $\widehat{\boldsymbol{\eta}}$ and $\xi(\mathbf{X}; \mathbf{u}_a)$ are replaced by their expressions given by Eqs. (16) and (27).



Let us apply in Eq. (34) the update rule $\dot{\hat{\eta}}_{1,k}$ (with $k = z, \phi, \theta, \psi, x, y = 1, 2, 3, 4, 5, 6$) given by Eq. (16) to obtain:

$$\begin{aligned} \dot{V} &= \text{tr}[\tilde{\eta}_1^T (\Gamma_{\eta} \dot{\hat{\eta}}_1 - I_6 s^T)] - \sum_{i=1}^6 K_i \frac{s_i^2}{\exp(s_i) + 1} + s^T \hat{\epsilon} I_6 - s^T \eta_2 I_6 \\ &= \sum_{k=1}^6 [\tilde{\eta}_{1,k} (\Gamma_{\eta,k} \dot{\hat{\eta}}_{1,k} - s_k)] - \sum_{i=1}^6 K_i \frac{s_i^2}{\exp(s_i) + 1} + s^T \hat{\epsilon} I_6 - s^T \eta_2 I_6 \tag{35} \\ &\leq \sum_{k=1}^6 [|\tilde{\eta}_{1,k}| (\Gamma_{\eta,k} \dot{\hat{\eta}}_{1,k} - |s_k|)] - \sum_{i=1}^6 K_i \frac{s_i^2}{\exp(s_i) + 1} + s^T \hat{\epsilon} I_6 - s^T \eta_2 I_6 \\ &= - \sum_{i=1}^6 K_i \frac{s_i^2}{\exp(s_i) + 1} + s^T (\hat{\epsilon} - \eta_2) I_6 \leq - \sum_{i=1}^6 K_i \frac{s_i^2}{\exp(s_i) + 1} + \|s\| (\|\hat{\epsilon}\| - \|\eta_2\|) \end{aligned}$$

By using the value η_2 expressed by Eq. (16) we obtain

$$\dot{V} \leq - \sum_{i=1}^6 K_i \frac{s_i^2}{\exp(s_i) + 1} + \|s\| \left(\frac{1}{\rho} - 1\right) \|\eta_2\|$$

With $K_i > 0$ and $\rho > 1$, we have $\dot{V} \leq 0$. Therefore, the closed-loop system is asymptotically stable despite uncertain dynamics, external disturbances and actuation faults. Hence, we conclude that the control objective is achieved when the proposed control law is used with the defined constant and dynamic parameters, as according to the Barbalat's lemma $e \rightarrow 0$ when $t \rightarrow \infty$.

V. SIMULATION RESULTS AND DISCUSSION

To illustrate the efficiency of the proposed quadrotor adaptive nonlinear FTC (QANFTC), here we present simulation results obtained using MATLAB/ SIMULINK. For benchmarking purpose, these results are compared to those obtained using the robust SOSMC developed in [1] for the quadrotor, which is implemented using known system parameters.

Parameters of the simulated UAV are given in table 1 [1, 13]. It is assumed that m_s represents the total weight of the UAV, which includes 1.1 kg for the UAV and 0.77 kg for the payload. The selected values for the controller's design parameters and for the RBFNN are given in table 2. For this simulation, initial values for positions and the Euler's angles are considered to be zero. The control objective is to track the reference positions and angles given in table 3.

Table 1: Parameters of the simulated quadrotor

Variable	Values	Units
m_s	1.87	kg
l	0.21	m
$l_x = l_y$	1.22	Ns^2/rad
l_z	2.2	Ns^2/rad
J_r	0.2	Ns^2/rad
$k_i (i = 1, 2, 3)$	0.1	Ns/m
$k_i (i = 4, 5, 6)$	0.12	Ns/m
g	9.81	m/s^2
b	5	Ns^2
k	2	Nm/s^2
C	1	-

Table 2: QANFTC and RBFNN parameters

Parameters	Values
$K_j (j = \phi, \theta, \psi, x, y, z)$	5
$c_j (j = \phi, \theta, \psi, x, y, z)$	5
$\rho_j (j = \phi, \theta, \psi, x, y, z)$	2.5
$\gamma_j (j = \phi, \theta, \psi, x, y, z)$	0.35
$\gamma_{\eta_j} (j = \phi, \theta, \psi, x, y, z)$	0.035
$\gamma_{\epsilon_j} (j = \phi, \theta, \psi, x, y, z)$	0.035
$\lambda_i (i = 1, 2, 3, 4, 5)$	0.1
$\beta_i (i = 1, 2, 3, 4, 5)$	0.5



Table 3: Desired positions and angles

Variables	Values	Time (in sec)
$[x_d, y_d, z_d]$	$[6.0, 6.0, 6.0]m$	$0 \leq t < 10$
	$[3.0, 6.0, 6.0]m$	$10 \leq t < 20$
	$[3.0, 3.0, 6.0]m$	$20 \leq t < 30$
	$[6.0, 3.0, 6.0]m$	$30 \leq t < 40$
	$[6.0, 6.0, 6.0]m$	$40 \leq t < 50$
	$[6.0, 6.0, 0.0]m$	$t \geq 50$
$[\phi_d, \theta_d, \psi_d]$	$[0.0, 0.0, 0.5]rad$	$0 \leq t < 50$
	$[0.0, 0.0, 0.0]rad$	$t \geq 50$

Table 4: Aerodynamics forces and torques

Disturbances	Values	Time (in sec)
$[d_x, d_y, d_z]$	$[0.0, 0.0, 0.0]N$	$0 \leq t < 15$
	$[0.0, 1.0, 1.0]N$	$15 \leq t < 20$
	$[1.0, 0.0, 1.0]N$	$20 \leq t < 50$
	$[1.0, 1.0, 1.0]N$	$t \geq 50$
$[d_\phi, d_\theta, d_\psi]$	$[0.0, 0.0, 0.0]Nm$	$0 \leq t < 50$
	$[1.0, 1.0, 1.0]Nm$	$t \geq 50$

To check robustness in case of external disturbances, we apply to the system, on the six degrees of freedom, disturbances that are the aerodynamics forces and torques given in table 4. Simulation results show that despite external disturbances on the six degrees of freedom the UAV tracks the desired trajectory with accuracy.

To check robustness in case of parameter changes, we consider that the UAV drops its load at $t = 40s$ such that m_s varies from $1.87kg$ to $1.1kg$.

To check robustness against actuation faults, we consider a scenario in which, at $t = 25s$, the first and third motors lose simultaneously 25% and 30% of their control effectiveness, respectively. In this scenario, it is also assumed that a 40% loss of effectiveness occurs in the second and the fourth motor at $t = 50s$. Simulation results depicted by Figs. 1, 2 and 3 show clearly that, with the designed controller, the UAV is able to stay perfectly in balance during flight when the load attached to it is dropped, when external disturbances and actuation faults occur for many motors. As illustrated by Fig. 1, a good tracking accuracy is obtained with the proposed QANFTC while the robust controller from [1] fails and leads to a crash at $t = 25sec$ due to actuator faults.

Figure 3 illustrates the UAV's trajectory in 3D when the two controllers are used. One can see clearly that despite multiple perturbations, the UAV remains in normal flight with the proposed controller (see Fig. 3 (a)), while it loses its balance and crashes with the SOSMC (see Fig. 3 (b)).

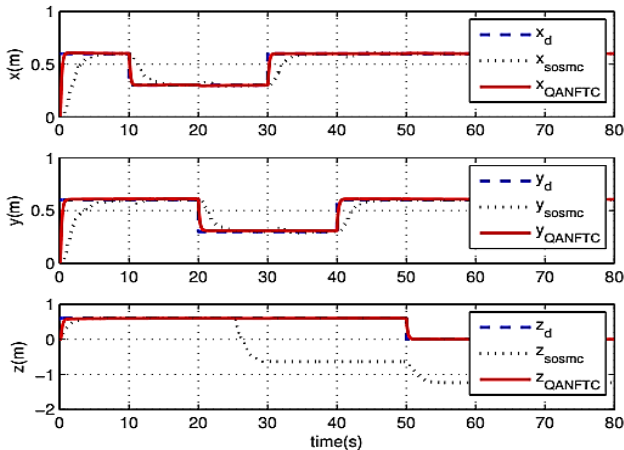


Fig. 1: x , y and z positions with the proposed QANFTC and with the robust SOSMC from [1] (with multiple perturbations).

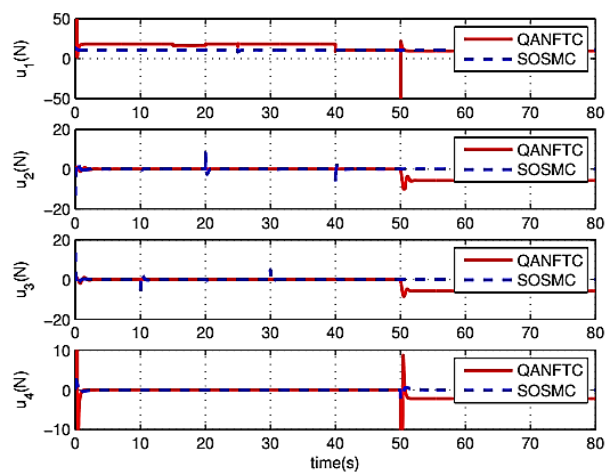


Fig. 2: Control signals u_1 , u_2 , u_3 and u_4 with the proposed QANFTC and with the robust SOSMC from [1] (with multiple perturbations).

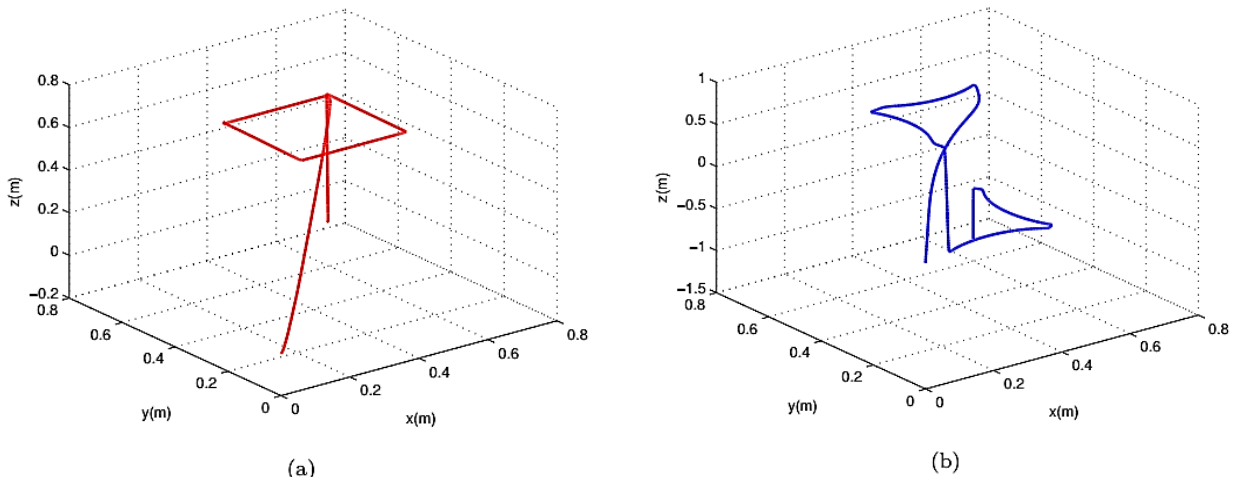


Fig. 3: 3D trajectory (a) with the proposed QANFTC(with multiple perturbations) and (b) with the robustSOSMC from [1]

VI. CONCLUSION

In this paper, an adaptive nonlinear controller has been designed for a six degree of freedom quadrotor unmanned aerial vehicle such that issues related to uncertain or varying parameters, external disturbances and multiple actuation failures can be tackled. Radial basis function neural networks have been used to provide approximation of uncertain dynamics and their update rule have been designed. To cancel the effects of external disturbances combined with those of actuation

faults, some dynamic parameters have been incorporated in the control law. Suitable update rules for these time varying parameters have been designed. Knowing that neural network approximation errors can also affect the control system performance, a dynamic parameter has been used for compensating the effects of these errors. Through AI Lyapunov stability analysis, it has been proved that the proposed control law with its dynamic parameters guarantee the closed-loop system stability while assuring that the control objectives are achieved. Results obtained with the proposed controller, under no perturbation condition, have been compared to those obtained with a robust second order sliding mode controller. It has been illustrated how under the aforementioned condition the proposed controller outperformed its counterpart. In order to illustrate the effectiveness of the proposed controller in severe operation conditions such as simultaneous multiple motor faults, aerodynamics forces and torques, simulation results have been presented. It has been shown that the proposed controller ensures very good tracking accuracy and a fast response despite simultaneous severe perturbations.

A future research could extend the proposed quadrotor's controller by integrating a state observer so that the use of some sensors could be avoided. Experimental validation of theoretical results presented in this paper could be performed as well.

REFERENCES

- [1] E. Zheng, J. Xiong and J. Luo, "Second order sliding mode control for a quadrotor UAV," ISA Transactions, vol. 53, pp. 1350-1356, 2014.
- [2] Z. Liu, C. Yuan and Y. Zhang, "Active fault-tolerant control of unmanned quadrotor helicopter using linear parameter varying technique," J Intell Robot Syst., vol. 88, pp. 415-436, 2017.
- [3] Y. Zhong, Z. Liu, Y. Zhang and W. Zhang, "Active fault-tolerant tracking control of a quadrotor with model uncertainties and actuator faults," Frontiers of Information and Electronic Engineering, vol. 20, pp. 95-106, 2019.
- [4] N. Ahmed and M. Chen, "Sliding mode control for quadrotor with disturbance observer," Advances in Mechanical Engineering, vol. 10, no. 7, pp. 1-16, 2018.
- [5] C. Nkouagnou, Haman, DJ and J. Aurelien, "Robust control of UAV coaxial rotor by using exact feedback linearization and PI-observer," Int. J. Dynam. Control, vol. 7, pp. 201-208, 2019.
- [6] A. S. Sudhir, "Decoupled control design for robust performance of quadrotor," International Journal of Dynamics and Control, vol. 6, pp. 1367-1375, 2019.
- [7] S. Zeghlache, K. Kara and D. Saigaa, "Fault tolerant control based on interval type-2 fuzzy sliding mode controller for coaxial trirotor aircraft," ISA Transactions, vol. 59, pp. 215-231, 2015.



- [8] Z. Li, X. Ma and Y. Li, “Robust tracking strategy for a quadrotor using RPD-SMC and RISE,” *Neurocomputing*, vol. 331, pp. 312-322, 2019.
- [9] B. Mushage, J. Chedjou and K. Kyamakya, “Observer-based fuzzy adaptive fault-tolerant nonlinear control for uncertain strict-feedback nonlinear systems with unknown control direction and its applications,” *Nonlinear Dyn.*, vol. 88, pp. 2553-2575, 2017.
- [10] B. Mushage, J. Chedjou and K. Kyamakya, “Fuzzy neural network and observer-based fault-tolerant adaptive nonlinear control of uncertain 5-DOF upper-limb exoskeleton robot for passive rehabilitation,” *Nonlinear Dyn.*, vol. 87, pp. 2021-2037, 2017.
- [11] S. Li, Y. Wang and J. Tan, “Adaptive and robust control of quadrotor aircrafts with input saturation,” *Nonlinear Dyn.*, vol. 89, pp. 255-265, 2017.
- [12] B. Wang, X. Yu, L. Mu and Y. Zhang, “Disturbance observer-based adaptive fault-tolerant control for a quadrotor helicopter subject to parametric uncertainties and external disturbances,” *Mechanical Systems and Signal Processing*, vol. 120, pp. 727-743, 2019.
- [13] H. Razmi, “Adaptive neural network based sliding mode attitude control for a quadrotor UAV,” *J. Cent. South Univ.*, vol. 25, pp. 2654-2663, 2018.
- [14] S. Zeglach, H. Mekki, A. Bouguerra and A. Djerioui, “Actuator fault tolerant control using adaptive RBFNN fuzzy sliding mode controller for coaxial octorotor UAV,” *ISA Transactions*, vol. 80, pp. 267-278, 2018.
- [15] S. Li, Y. Wang, J. Tan and Y. Zheng, “Adaptive RBFNNs/integral sliding mode control for a quadrotor aircraft,” *Neurocomputing*, vol. 216, pp. 126-134, 2016.
- [16] R. Avram, X. Zhang and J. Muse, “Nonlinear adaptive fault-tolerant quadrotor altitude and attitude tracking with multiple actuator faults,” *IEEE Transactions on control systems*, vol. 26, pp. 701-708, 2018.